Practical Descattering of Transmissive Inspection Using Slanted Linear Image Sensors

Takahiro Kushida[1] Kenichiro Tanaka[1,2] Takuya Funatomi[1] Komei Tahara[3]
Yukihiro Kagawa[3] Yasuhiro Mukaigawa[1]

[1]Nara Institute of Science and Technology
8916–5 Takayama-cho, Ikoma, Nara 630–0192, JAPAN
{kushida.takahiro.kh3, ktanaka, funatomi, mukaigawa}@is.naist.jp
[2]Ritsumeikan University
1–1–1 Noji-higashi, Kusatsu, Shiga 525–8577, JAPAN
ken-t@fc.ritsumei.ac.jp
[3]Vienex Corporation
262 Yoshioka-cho, Kanonji, Kagawa 768–0021, JAPAN
{komei_tahara, yukihiro_kagawa}@vienex.co.jp

Abstract

This paper presents an industry-ready descattering method that is easily applied to a food production line. The system consists of multiple sets comprising a linear image sensor and linear light source, which are slanted at different angles. The images captured by these sensors, which are partially clear along the perpendicular direction to the sensor, are computationally integrated into a single clear image over the frequency domain. We assess the effectiveness of the proposed method by simulation and by our prototype system, which demonstrates the feasibility of the proposed method on an actual production line.

1 Introduction

Foreign-object inspection for food production lines is important for preserving the safety of products. Inspection is required to be both fast and non-destructive, to increase the productivity of a food factory. A typical approach is to put a light source and a detector on the opposite sides of an object to see through the object; however, the captured images are blurred because of the scattering of the light. In this paper, we aim to obtain a clear image of the transmissive observation that is suitable for an existing production line.

One of the traditional approaches for image restoration is a deconvolution approach, whereby some priors on the scene and the kernel are assumed [1, 2, 3, 4]. Unfortunately, the quality of the recovered image is generally low because of the loss of high-frequency components during the observation process. Another approach is to use a projector–camera system [5, 6, 7, 8] to probe the light transport. Although the image quality is very high with this approach, it requires multiple observations of the same scene; hence, it is not straightforward to apply it to a production line. We take a hybrid approach that is suitable for a production line and conserves high-frequency detail.

In our approach, we simply use multiple sets comprising a linear image sensor and linear light source, which are already used on the production lines. The key point is that the sets of sensors and light sources are slanted relative to the direction of the conveyor. For each sensor, it is possible to obtain an image of the moving subject by stacking the observations. This image is blurred along the sensor direction but clear along the perpendicular direction. Using different anisotropically clear images, we can computationally recover a totally clear image.

The chief contribution of this paper is that it presents the first industry-ready descattering method. Our method can easily be applied to an production line without any new components, simply by placing two traditional linear sensors, each rotated by ±45 degrees.

2 Line-scan imaging on a conveyor system

Line-scan imaging is common on production lines because of its efficient mechanism. The imaging device consists of a linear image sensor and linear light source and outputs a single row of pixels per exposure. As the objects on the conveyor pass in front of the sensor, a two-dimensional(2D) image can be obtained by stacking the captured rows, one by one, as shown in Fig. 1.

A foreign object inspection usually observes the light transmitted through the scanned subject. The light that straightly passes straight through the subject forms a clear shape of the foreign object; however, there is also scattered light, which blurs the image and

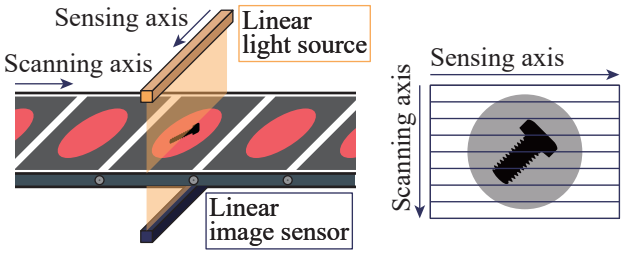

Figure 1. Line scan imaging . A set, comprising a linear light source and linear image sensor, is installed on each side of a conveyor. Subjects move on the conveyor, and the linear image sensor measures the light transmitted through the subjects. A 2D image is obtained by stacking the linear images.

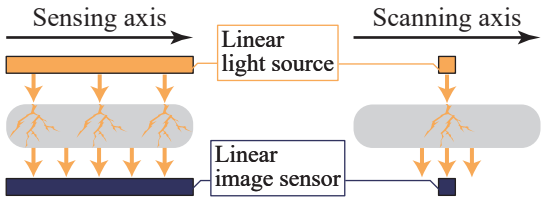

Figure 2. Anisotropic descattering effect on line-scan imaging. The scattered light is captured along the sensing axis but not along with the scanning axis.

makes it difficult to recognize the presence of the foreign object.

Because the scattering is diffusive, the blur is isotropic in common 2D area imaging, whereas it appears differently in line-scan imaging because of its anisotropic illumination and sensing, as shown in Fig. 2. The blur is similar to that of area imaging along the sensing axis but less scattered light exists along the scanning axis.

3 Descattering with multiple slanted linear image sensors

In a single observation with the linear light source and linear image sensor, the scattering blur still exists along the sensing axis. We aim to develop a method of isotropic descattering, from multiple partially descattered observations, that is suitable for production lines. To obtain the multiple images, the observations of each object must be conducted at different orientations. However, physically rotating the subject may degrade productivity. Our key idea is a co-design of hardware and algorithm. We use multiple sets comprising a linear light source and linear image sensor slanted at different angles (Fig. 3) and to computationally integrate the multiple observations into one image (Fig. 4).

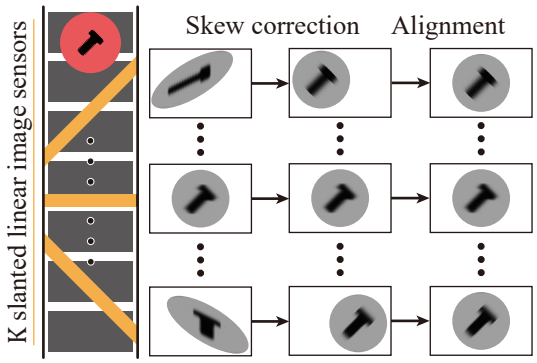

Figure 3. Multiple slanted linear image sensors for line-scan imaging. The observed images are corrected and aligned.

3.1 Multiple slanted linear image sensors

We use multiple sensors to obtain differently blurred images without rotating the subjects, to maintain productivity. To enable subjects to keep moving along the production line, we install the linear light sources and linear image sensors slanted from the scanning axis, as shown in Fig. 3. Suppose that we wish to sample at K angles evenly. In line scanning, there is a restriction that the sensing axis must not be identical to the scanning axis, or a 2D image cannot be obtained. Therefore, we set the angle between the sensing and scanning axes to be

$$\theta_k = \frac{2k+1}{2K}\pi, \tag{1}$$

where $k = 0, \cdots, K-1$.

Because the sensing and scanning axes are not orthogonal, the 2D images obtained may be skewed. We correct the skew in the 2D images according to the moving speed of the subject and the sensor bandwidth. Alignment of the observations is necessary for the integration. This is possible by adjusting the synchronization of the sensors according to the moving speed of the subject. However, in this study, we placed some markers at known positions to achieve the alignment without the need for engineering work.

3.2 Image integration based on maximum Fourier amplitude spectrum

We propose a method to recover a clear image from the K observations with anisotropic blur, as shown in Fig. 4. We formulate the blurring in the Fourier domain to cope with this anisotropicity.

We first consider the isotropic case. Suppose that the isotropic blur is caused by diffusive scattering and is spatially invariant. The blurring process is formulated as a convolution of a clear image $f(x, y)$ and Point

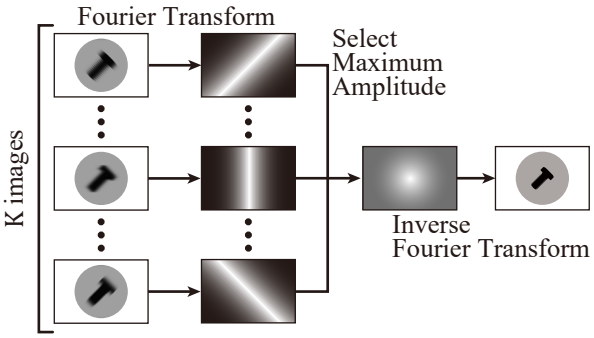

Figure 4. Integration in the Fourier domain. Applying Fourier transform to the observed images, K images are obtained. For each frequency in the Fourier-transformed image, the component with the maximum amplitude among the K images is selected and integrated into a single image. The integrated clear image is recovered by applying inverse Fourier transform.

Spread Function (PSF) $h(x, y)$ [1].

$$g(x, y) = f(x, y) * h(x, y), \tag{2}$$

where $g(x, y)$ is the blurred image and $*$ is a convolution operator. The PSF depends on the properties of the scatterer, such as its material and thickness. It also depends on the imaging process. When the scattering is diffusive, $h(x, y)$ is isotropic in standard area imaging.

However, it becomes anisotropic when a linear image sensor and light source are used. The PSF is formulated as a function of the angle θ of the sensing direction. The k-th observation, with angle θ_k, is formulated as,

$$g_k(x, y) = f(x, y) * h_k(x, y). \tag{3}$$

In the Fourier domain, the blurring process is interpreted as a decay of the high-frequency components. In isotropic blurring, the high-frequency components of the $\mathcal{F}[h(x, y)]$ are close to zero, where $\mathcal{F}$ denotes the Fourier transform operator. In addition, the high-frequency components of $\mathcal{F}[h_k(x, y)]$ are small along the sensing direction. Therefore, each of the anisotropic images maintains the high-frequency components along a different direction. If they can be complementary to each other, the blur can be mitigated by aggregating the remaining high-frequency components. As the aggregation operator, we adopt max in the Fourier domain.

Applying the Fourier transform to Eq. (3), the equation becomes

$$\begin{aligned} \mathcal{F}[g_k(x, y)] &= \mathcal{F}[f(x, y) * h_k(x, y)] \\ G_k(u, v) &= F(u, v) H_k(u, v), \end{aligned} \tag{4}$$

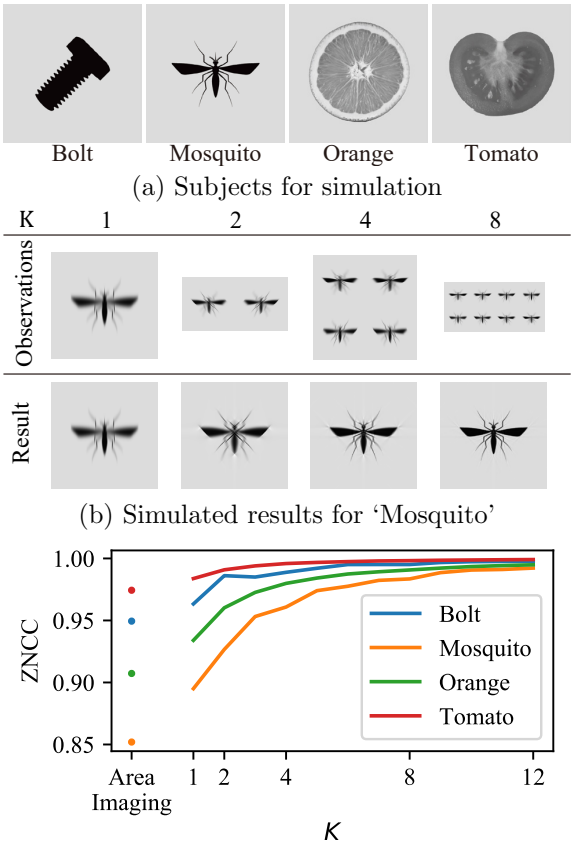

(a) Subjects for simulation

(b) Simulated results for 'Mosquito'

(c) ZNCC vs K

Figure 5. Performance analysis by simulation.

where G, F, and H are the Fourier transforms of g, f and h, respectively. For each pixel (u_0, v_0) of the integrated image in frequency domain $\hat{G}$, we assign the component with the maximum amplitude among the K images.

$$\begin{aligned} \hat{G}(u_0, v_0) &= G_{k'}(u_0, v_0) \\ k' &= \arg\max_k |G_k(u_0, v_0)| \\ &\forall (u_0, v_0) \in (u, v). \end{aligned} \tag{5}$$

Finally, the integrated clear image $\hat{g}$ is obtained by applying the inverse Fourier transform:

$$\hat{g}(x, y) = \mathcal{F}^{-1}[\hat{G}(u, v)]. \tag{6}$$

4 Simulation

The performance of the descattering depends on the number of observations. We clarified the relationship between them by simulation. We simulated line-scan imaging by convolving a blur kernel onto a clear image of size 512×512, using Eq. (2). To simulate the blur

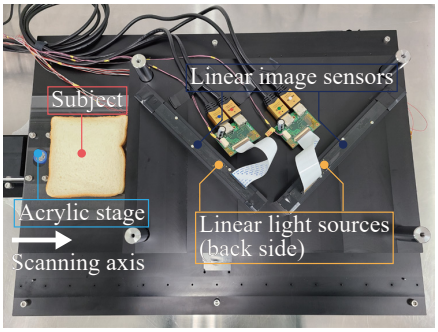

Figure 6. Prototype system.

in the k-th observation, we applied a 1×63 rectangular window mask, slanted at an angle of θ_k, for an isotropic 2D Gaussian blur kernel with $\sigma = 21$ in the spatial domain. We also simulated the blurred image with the kernel without masking, which corresponds to observation using area imaging, for reference. We evaluated the descattering performance by calculating the zero-normalized cross-correlation (ZNCC) between the clear and recovered images.

The results are shown in Fig. 5. We used the four images shown in Fig. 5(a). Figure 5(b) shows the observations from simulated line-scan imaging and the recovered image for various numbers of observations: $K = 1, 2, 4$, and 8. Figure 5(c) shows the ZNCC for area imaging and for line-scan imaging with $K = 1, \cdots, 12$.

The results show that the ZNCC for line-scan imaging, even with $K = 1$, is significantly better than that for area imaging. They also show that the ZNCC depends on the subject. The proposed method is more effective for complex-shaped and high-contrast subjects, such as 'Mosquito' and 'Orange.' Generally, increasing the number of observations K improves the quality of the recovered image. The benefit becomes smaller as K increases, whereas the cost increases linearly with K. Therefore, $K = 2, 3$ would be ideal for practical use.

5 Prototype system

We developed a prototype system with two pairs comprising a linear image sensor and near infrared light source, as shown in Fig. 6. The sensors were installed in the system rotated by ±45 degrees.

Figure 7 shows the observations and preprocessing for a white acrylic plate with a black plastic piece. The left column shows that the captured images are skewed and misaligned. The preprocessing described in Sec. 3.1 was executed to correct the skew and align the images as shown in the middle column. The right column shows the result of the proposed method.

We measured foreign objects in real foods as shown in Fig. 8. Three black plastic pieces were used as foreign objects, and a cracker and a slice of bread were

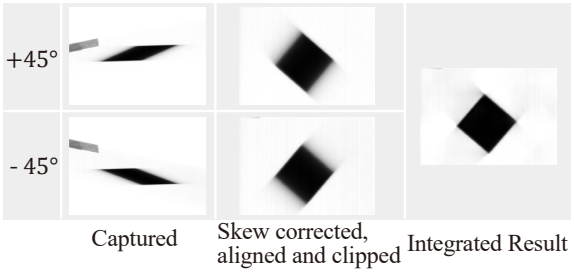

Figure 7. Images from two linear image sensors and the result of the proposed method. Left: The subject is skewed and misaligned in the captured images. Middle: Skew correction and alignment have been applied. Right: Result of proposed method.

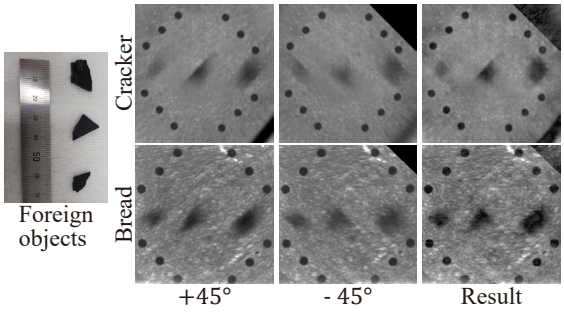

Figure 8. Results with real food, showing that our proposed method worked successfully in the prototype system and high-frequency detail was obtained.

placed on these objects. The results show that the foreign objects were significantly blurred along the sensing axis in each of the captured images. However, the proposed method worked successfully to clarify the silhouettes of the foreign objects in the real foods.

6 Conclusion

In this paper, we propose a co-design of hardware and algorithm for foreign object inspection. The design can easily be installed in a production line with line-scan imaging. It enables a clear image to be obtained by computationally integrating multiple line-scan images slanted at different angles. We assessed the effectiveness of the proposed method by simulation. We also constructed a prototype system, which demonstrated the feasibility of the proposed method on an actual production line.

Acknowledgment

This work is partly supported by JST CREST JPMJCR1764.

References

[1] S. G. Narasimhan and S. K. Nayar, "Shedding light on the weather," in *2003 IEEE Computer Society Conference on Computer Vision and Pattern Recognition, 2003. Proceedings.*, vol. 1, pp. I–I, 2003.

[2] S. Metari and F. Deschenes, "A New Convolution Kernel for Atmospheric Point Spread Function Applied to Computer Vision," in *Proc. International Conference on Computer Vision (ICCV)*, (Rio de Janeiro, Brazil), pp. 1–8, IEEE, 2007.

[3] C. Fuchs, M. Heinz, M. Levoy, H.-P. Seidel, and H. P. A. Lensch, "Combining Confocal Imaging and Descattering," *Computer Graphics Forum*, vol. 27, pp. 1245–1253, June 2008.

[4] R. Wang and G. Wang, "Single image recovery in scattering medium by propagating deconvolution," *Optics Express*, vol. 22, p. 8114, Apr. 2014.

[5] S. Seitz, Y. Matsushita, and K. Kutulakos, "A theory of inverse light transport," in *Proc. International Conference on Computer Vision (ICCV)*, pp. 1440–1447 Vol. 2, 2005.

[6] S. K. Nayar, G. Krishnan, M. D. Grossberg, and R. Raskar, "Fast separation of direct and global components of a scene using high frequency illumination," *ACM Tran. on Graphics (ToG)*, vol. 25, pp. 935–944, July 2006.

[7] K. Tanaka, Y. Mukaigawa, Y. Matsushita, and Y. Yagi, "Descattering of transmissive observation using Parallel High-Frequency Illumination," in *Proc. International Conference on Computational Photography (ICCP)*, pp. 1–8, Apr. 2013.

[8] M. O'Toole, S. Achar, S. G. Narasimhan, and K. N. Kutulakos, "Homogeneous codes for energy-efficient illumination and imaging," *ACM Tran. on Graphics (ToG)*, vol. 34, pp. 1–13, July 2015.